Design Analysis of a Shallow Water Mooring System for Tanker Vessel

Duke Omiete Dagogo, Ibiba Emmanuel Douglas and Tamunodukobipi Daniel

Marine Engineering Department, Rivers State University, Port Harcourt, Rivers State Nigeria.
Corresponding Author: Duke Omiete Dagogo

ABSTRACT: *This study develops a virtual tool for predicting ship motions and tension in mooring line to facilitate mooring line materials selection for tanker vessel. Basic ship motion and wave theories are applied to describe the tanker behavior in uncoupled roll, and coupled heave and surge motions, respectively. The hydrodynamic potentials of added mass and damping coefficients of the various modes of motions, their retardation functions, and the total excitation forces are determined using numerical techniques. This is imperative for preliminary ship design for good seakeeping performance. Froud-krylov forces, restoring and diffraction forces for coupled heave, surge and uncoupled roll are characterized. The solutions of the response amplitude operators obtained are validated against AnsysAqwa: and the results are in reasonably good agreement.*

KEY WORDS: Froud-Krylor Force, Response Amplitude Operator, Responses, Mooring Lines, Frequencies.

I.   INTRODUCTION

Loading operation with vessel requires lots of experiences and skills to ensure good stability, safety and efficiency. The vessel may experience lots of dynamic loads. These dynamic loads can be wave load, wind load and dynamic effect due to cargo loading at midstream.Ofall these, the latter has the severest effect on the vessel. A good mooring system is needed to keep the vessel in position irrespective of the severity of the environmental loads. To design such a mooring system that can withstand these dynamic loads, the total load on the entire system must first be determined,and the dynamics responses of the vessel based on the six degrees of freedomcan then be computed.The six degrees of freedom of motion of the vessel are:three linear (that is Heave, Surge and Sway),and three rotational (Pitch, Roll and Yaw), respectively.

For analysis of the dynamic response of the vessel, these motions are classed as coupled and uncoupled, with the linear movement representing the uncoupled, whilethe combination of one linear and a rotational movement representing the coupled. So, to design a mooring system for a vessels or offshore structures, these dynamic loads and their axes should bedetermined precisely. This is required for calculating theresultanttotal load on any axisof the mooring system,as it produces the torque and tension that can sufficiently counter the effect of the dynamic loads on the vessel or offshore structure.In this research, the dynamic loads on the tanker vessel are limited to those that can cause only three degrees of uncoupledmotion.

Mooring lines

Huang and Vassalos[1] presented a numerical lumped-mass model for predicting snap loads on marine cables operating in alternating taut-slack conditions. They note that the possibility of a cable becoming slack exists whenever the tension temporarily falls to a level which is comparable to the distributed drag force along the cable. In this circumstance and with the prevalence of periodic environmental loadings, the cable would operate in alternating taut-slack conditions. Moreover, depending upon the rate at which the cable becomes taut, the transition from the slack to the taut state may cause a momentarily high tension in the cable. The resultant stress may be too large as to even cause cable breakage.

The researchers opined that when the cable was under severe excitation (an amplitude of 0.075 m and a frequency of 1 Hz), the response becomes distorted. The displacement was characterized by sharp troughs and flat crests, while the velocity had flat troughs and sharp crests. The magnitude of the

acceleration became much larger since the transition from slack to taut states involved a sudden change in velocity. Similarly, Cozijn and Bunnik[2]showed that the mooring system contributes to the inertia and the damping of a CALM

buoy's surge motion. It was observed that the inertia effects were functions of the mass and added mass of the mooring lines and export risers, which moved with the CALM buoy. Whereas, the damping effects were consequence of the drag loads on the mooring lines and export risers.

In furtherance, Hall, et al [3]established that drag from the mooring lines could contribute significantly to the overall damping on floating wind turbine platforms – typically in the order of 5% of total damping in most degrees of freedom. Zhu et al [4] developed a simulation model for a deep-sea tethered remotely operated vehicle. It was shown that the cable tension was sensitive to surge motion when the ship was located upstream of the remotely operated vehicle (ROV), and sensitive to heave motions when the ship was located downstream of the ROV. Zhu et al [5] formulated three-dimensional equations of motion for a marine tethered ROV system that support large elastic deformations and snap loads, using the lumped parameter approach. It was shown that the snap loads increased as the stiffness of the sling increased, up to even beyond the cable breaking strength. Conversely, at low flow speeds, the snap loads were reduced. From their results, it can be deduced that the tether tension increases significantly as the speed of the current increases.

Lu et al [6] investigated the dynamics of submerged floating tunnels supported by taut lines including snap loads on the tethers. The sensitivities of extant slack tether to wave height and wave period were probed. The study revealed that at large wave heights, a submerged floating tunnel tether could become slack and experience snap loads during re-engagement. A complementary study by Han et al [7]indicated that an entire mooring system was liable to fail suddenly once the most severely loaded line was broken. This is consistent because such a break induces a large offset of the floating structure, which causes sharp increase of tensile stress in the adjacent mooing lines. This eventually leads to the successive failure of the mooring system.

Consequently, Masciola et al [8] studied the influence of mooring line dynamics on the response of a floating offshore wind turbine, and compared the results against an equivalent uncoupled mooring model. It was observed that the coupled and uncoupled platform responses differed when snap loads occurred. The time lag between a loss of cable tension and a snap load was short, but significant enough to affect the outcome of the results. It was also noted that a snap load results in a large force being applied to the platform due to rapid cable re-tensioning. This phenomenon explains why large differences occur between the coupled and uncoupled models in regions near snap loads.

Vessel Motions History Before the 1980s'

The strong, watertight construction and durability attributes of floating structures, structurally enable them to survive rough water. Sea worthiness is a prime consideration during design and operation as to withstands the violent wave forces and render them kindly to both the vessel, its crew members and operations. Sea-kindliness, habitability and spaciousness for crew members- were not given serious concerns over the centuries until there were issues on sea transportation, ranging from capsizing, collision, grounding, to other safety related incidents such as fire[9].

To enhance the seaworthiness of floating structures, Salvesen and Tucks evolved the strip theory to make relevant improvement in marine ship building technology today [10]. The strip theory divides the ships' profile views into two-dimensional body plans and determining its hydrodynamic properties such as the added masses and damping for the different modes of freedoms. The strip theory when combined with Conformal mapping techniques can be implemented to address ship vibration problems. Another method for computing the added mass and damping is the Frank Pulsating source theory, which uses the highly rigorous green theorem. All of these techniques were cumbersome to carry out by computations by hand, even though their predictions reasonably agree with test data. Ship hydrodynamics is an essential and ongoing research. A substantial amount of work has been carried out to determine the hydrodynamic characteristics of hulls [8]. Hull displacements under complex loading conditions are difficult and often impossible to predict precisely [11]. Understanding how a hull will behave under limited and controlled conditions renders insight into how a hull may displace in more complex situations.

The researchers proposed a method for determining the added mass moment of inertia for various hull shapes, setting the former as a function of the shape of the hull under consideration. Conformal transformation based on a circle was employed to approximate actual ship sections. Vugts[12] applied theoretical and experimental techniques to determine the hydrodynamic coefficients of two-dimensional cylinders undergoing forced oscillations, heaving, swaying and rolling in a free-surface, respectively. The influence of section shapes on the coefficients were observed. Differences between the theoretically and experimentally obtained coefficients for sway and roll were evident. Viscous effects were distinctly

presented in the results. A complete set of hydrodynamic quantities for motions of cylinders in forced and in beam waves were analyzed.

Bishop et al [13] presented a potential flow solution using conformal mapping and a multiple potential flow method expansion. With this method two-dimensional hydrodynamic properties were computed for cylinders swaying and rolling in the free-surface of an infinite ideal fluid. Ikeda[14]proposed a simple method to predict the roll damping of ships by considering contributions from friction, wave, eddy, lift and bilge keel components. The numerical solution was compared against test data, and a good correlation was achieved. Floquet theory (for solving linearized differential equations) was implemented by Muik and Falzarano[15] to solve the six degreesoffreedomnon-linearshipmotions.Bifurcationandstabilitybehaviour of the coupled roll were studied. The linear three degrees of freedom and the associated non-linear coupling of roll, yaw and pitch results were compared. Concluding the article, the researcher opined that for comprehensive description of ship motions, all six degrees of freedom should be studied simultaneously.

Heave and sway motions are well predicted with potential flow and other theoretical methods. Roll behaviour is difficult to predict because of non- linearities. Often, Reynolds Averaged Navier-Stokes (RANS) based turbulence modeling methods are used to characterize the averaged properties of flow. In fact, avast majority of turbulent flow (for engineering applications) computations have been carried out with procedures based on the RANS equations [16]. A theoretical method of determining the hydrodynamic forces on an oscillating rectangular cylinder was proposed by Yeung et al [17]. Flow in the presence of a free-surface was modeled with a Free-Surface Random-Vortex Method (FSRVM). The vertical part was solved with the Random-Vortex Method (RVM) and the irrotational part with a complex-variable Boundary Element Method (BEM).

In the RVM, the vorticity y i eld was approximated by a collection of regions of concentrated vorticity in the flow yield. The FSRVM was validated by modelling a plate rolling in water and comparing it to experimental data [18]. This method was also applied to a horizontal circular cylinder translated through a fluid and with a rectangular cylinder heaving a free-surface [19]. Yeung et al[17] carried out an experiment for geometrically similar bottom hulls, and showed that scale discrepancy hadan effect on the results. However, both the FSRVM and experimental results of similar vessels did not fully agree with those presented by Vugts. Reasons for this are unclear. The FSRVM's predictions appear to be lacking in lower frequency oscillations (it is not stated what may be needed as a "low" frequency). It can be suggested that theFSRVM model predictive accuracy would improve by incorporating turbulence modelling.

Korpus and Falzarano[20] produced data by applying RANS methods to rolling ship sections. Only rectangular ship section (at-bottom-hull) under forced oscillations for heave, sway and roll was considered without the presence of a free-surface. Various roll amplitudes, oscillating frequencies and scales were investigated. Their panel code could not predict damping components satisfactorily. Finally, a rolling rectangular section in a free-surface, modeled with a RANS-based technique, was carried out by Sarkar and Vassalos[21]. Results were compared to available numerical and experimental data. This technique predicted damping and added moment of inertia coefficients more accurately than potential flow calculations could. The RANS-technique resolved the main characteristics of the rolling motion.

Rectangular sections (at-bottom hulls) are investigated more often than other ship sections because of their frequent commercial usage. Flow around floating production storage and loading (FPSO) hulls in roll were investigated by Kinnas et al [22]. A two-dimensional unsteady-flow Navier-Stokes solver was used. The results

were compared to that of a BEM based potential flow solver. The effect of turbulence for a submerged hull subject to alternating flow was investigated, using the commercial CFD code FLUENT.

The Reynolds stress model (RSM) with standard wall functions was applied. The difference between the results from turbulent flow and laminar flow in FLUENT were found to be negligible. Roll moment is highly non-linear with respect to angle of roll, since the former increases exponentially as the roll angle rises.

Chen and Liu[23] implemented non-dimensional RANS equations for this incompressible flow problem. The study also investigated the flow characteristics around a three-dimensional hull for initial roll angles of $5°$, $10°$ and $20°$. The hull was sub-divided and the flow characteristics for the different hull cross sections (two-dimensional) were determined. Furthermore, Wilson et al [24] investigated the rolling of surface combatants (in three dimensions), and validated the results via uncertainty analysis. Theirmodel accurately predicted seakeeping characteristics for typical hull-sections, with the aid of orthogonal curvilinear coordinates and a moving mesh formed around the hull. Their work illustrates the flow phenomenon around the different hull geometries and also the hull characteristics. However, their predictions were not directly compared with experimental data.

Kim[25]applied different numerical models to simulating the dynamic of surface ship, with specific application to the non-linear rolling of ship hull sections. This work was complemented by the development of ahighly non-linear ship model program, the Digital Self-Consistent Ship Experimental Laboratory (DiSSEL),[26]. Bilge-keel effects on the roll damping were easily investigated. The results obtained with this DiSSEL were in agreement with experimental results. Ship hull forms and geometry above the calm water line were also found to play a role in damping. Different definitions for the roll damping were presented.

Following this, a commercial RANS solver (ANSYS-CFX 10.0) was used to model two-dimensional cylindrical sections in heave, sway and roll [27]. Subsequently, the Shear Stress Transport (SST) turbulence model was developed by Menter and applied to circular and rectangular sections oscillated at frequencies of 1-12 rad/s in an initially undisturbed free-surface. Small displacement amplitudes were considered to compare the hydrodynamic coefficients to potential flow theory. Grid independence was achieved for all cases [27]. A good agreement between the numerical and experimental hydrodynamic coefficients [12].For the rolling rectangle, grid size, grid structure and time step size strongly influence the damping coefficients. Vortex shedding is suspected as the cause of the discrepancies between the numerical results for the roll case.

A direct method for solving the Navier-Stokes equations using the Nitevolume method was presented [28]. This method accounted for non-linear free-surface conditions. The model's effectiveness in resolving the effects of vortices on rolling barges with bilge-keels were tested. Vorticity contours and roll hydrodynamic coefficients were calculated from velocity and pressure yields. Small roll angles (less than 0.14 rad) were tested as the draft of the sections were relatively shallow compared to the half width of the barge. Vortex separation was found to contribute substantially to the damping force. Potential flow theory over-predicted the roll motion. Ibrahim and Grace[29] carried out different research on the yield of ship hydrodynamics using fundamental ship theory. Ship roll dynamics, stochastic roll stability and probabilistic roll dynamics were investigated. From the literature it is evident that ship hydrodynamics has a long research history and is still being expounded. With the advent of advanced numerical methods and highly sophisticated computing devices, large displacement ship motions simulation and properties predictions are done more accurately.
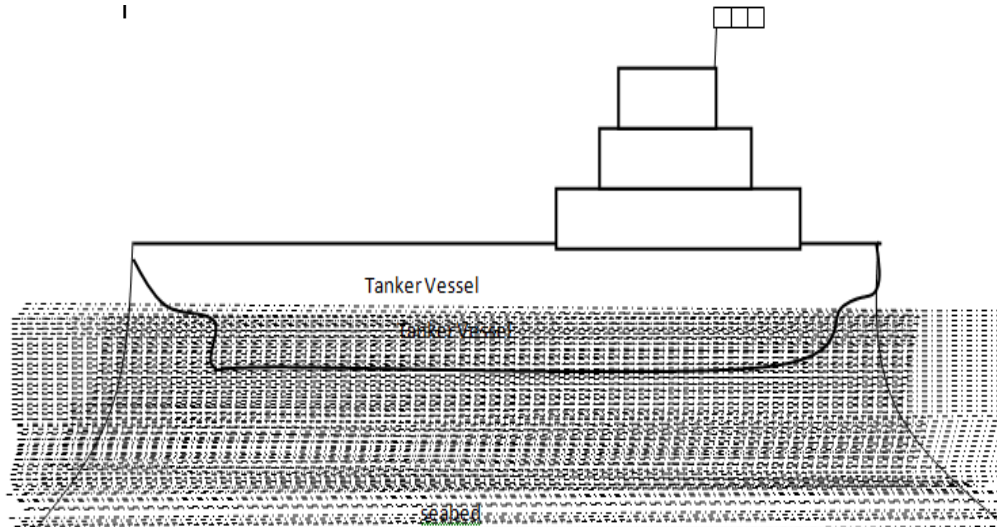
II.   MATERIALS AND METHODS

Figure 1: Schematic Diagram of a Moored Shuttle Tanker

Analytical Development of the Model.
This section entails the stepwise development of the analytical model used for the determination of the various parameters for the hydrodynamic design and analysis.

Section Mapping Coefficient sand Force Equations

$$H_0 = \frac{D_s}{2 \times D_s} \qquad\qquad (1)$$

Also, the sectional area of the section computed using the trapezoidal rule

$$\sigma_s = 2\left[\frac{\Delta Z}{2}\left(y_0 + y_n + 2\left(y_1 + y_2 + y_3 + y_4 + y_5 + \dots\dots y_{n-1}\right)\right)\right] \quad (2)$$

$$C = 3 + \frac{4\sigma_s}{\pi} + \left(1 - \frac{4\sigma_s}{\pi}\right)\left(\frac{H_0 - 1}{H_0 + 1}\right) \quad (3)$$

$$a_3 = \frac{C + 3 + \sqrt{9 + 2c}}{C} \quad (4)$$

$$a_1 = \frac{(H_0 - 1)(H_0 - a_3)}{1 + H_0} \quad (5)$$

and,

$$M_S = \frac{B_S}{2(1 - a_1 + a_3)} \quad (6)$$

Where,

$H_0 \rightarrow$ the Sectional draft to depth ratio.

$D_s \rightarrow$ the draft of the section considered.

$\Delta_z = Z_1 - Z_2$

$B_s \rightarrow$ sectional beam of the considered cross section

a_1, a_3, $\rightarrow$ initial computational coefficients,

$M_S \rightarrow$ the initial scale factor,

So, with the initial computation of a_1, a_3, and all other coefficients a_{2n-1}, from $n = 0$ to $n = end$, are set to zero. The iteration for solving the proper angle that maps each offered point in the ship is a complex plane to a unit circle start. This angle is computed using the set of equations.

$$x_i \times Cos\theta_i + M_s Cos\theta_i \sum_{n=0}^{N} a_{2n-1} Sin((2n-1)\theta) - y_i Sin\theta_i +$$

$$M_s \times Sin\theta_i \sum_{n=0}^{N} a_{2n-1} \times Cos((2n-1)\theta) = 0 \quad (7)$$

$$Cos\theta_i = \frac{x_{i+1} - x_{i-1}}{\sqrt{(x_{i+1} - x_{i-1})^2 + (y_{i+1} + y_{i-1})^2}} \quad (8)$$

and

$$Sin\theta_i = \frac{-y_{i+1} + y_{i-1}}{\sqrt{(x_{i+1} - x_{i-1})^2 + (y_{i+1} + y_{i-1})^2}} \quad (9)$$

In other to solve equation (7), put back equations(8) and (9), into equation (7)to get a set of equation in the form of $(AX = B)$=0. Note that the newvalue of M_S and a_{2n-1} are substituted into equation (7) to solve for new mapped angle.This repetitive iteration continues until certain design condition are met.The conditions are;

$$\Delta E = (L+1) \left[0.000005 \left(d_{max}^2 + b_{max}^2 \right) \right]^{1/2} \qquad (10)$$

$$e_i = (x_i - x_{0i})^2 + (y_i - y_{0i})^2 \qquad (11a)$$

and

$$x_{0i} = -M_s \sum_{n=0}^{N} (-1)^n \times a_{2n-1} \times \sin\left((2n-1)\,\theta\right) \qquad (11b)$$

$$y_{0i} = M_s \sum_{n=0}^{N} (-1)^n \times a_{2n-1} \times Cos\left((2n-1)\theta\right) \qquad (11c)$$

Where: d_{max}→ the maximum draft of the section
b_{max}→the maximum beam of the cross section

$$\Delta E = \sum_{i-0}^{I} \ell_i^2$$

Once the design condition or equation (10) is fulfilled, the values of M_S, a_{2n-1} can be obtained.

$a_{-1} = 1.00$, Hence at of $n = 0 \Rightarrow M_s \times a_{-1} = M_s \times 1$

Note that all the values or coefficients of $a_1, a_3, a_5, a_7 \dots \dots a_{2n-}$ can be obtained by dividing the solution by M_s.

Computing the Heave Force

$$(M + A_{33})\int_3 + B_{33} \int_3 + C_{33} \int_{33} = F_3 \, \ell^{iwet} \qquad (12)$$

However, these coefficients can be found as

$$A_{33} = \int a_{33} \, d\gamma \qquad (13)$$

$$B_{33} = \int b_{33} \, d\gamma \qquad (14)$$

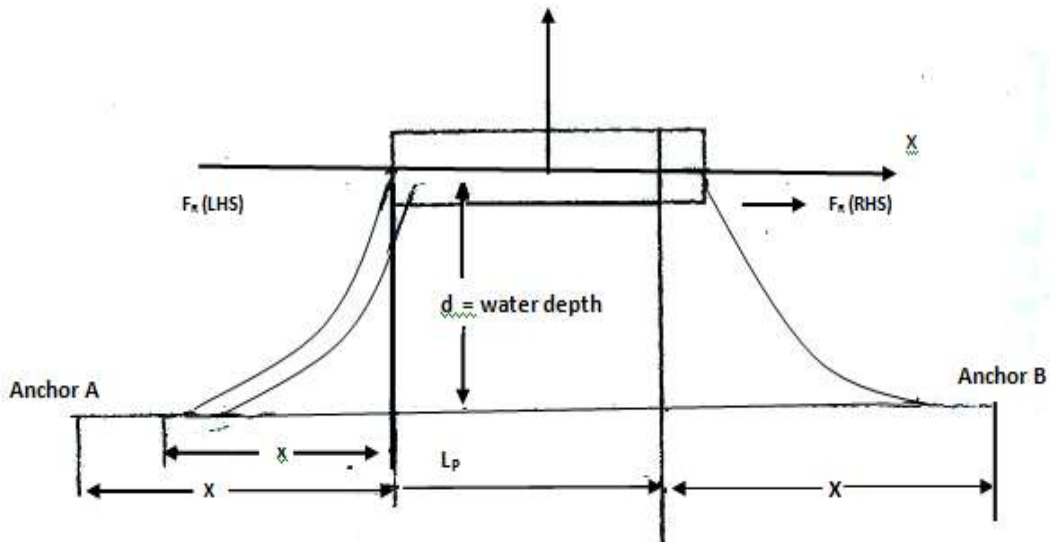$$C_{33} = \rho g \int b d\gamma = \rho g A_W \qquad (15)$$

Figure 2: Free body diagram of a catenary moored tanker vessel.

Suspended line length (L$_s$)

$$L_s = a \sinh\left(\frac{x}{a}\right) \tag{16}$$

Vertical dimension (depth = h)

$$h = \left[\cosh\left(\frac{x}{a}\right) - 1\right] \tag{17}$$

combing equations (16) and (17) yields

$$L^2_s = h^2 + 2ha \tag{18}$$

Using line Tension at the platform, tension at the top

$$T = w\frac{\left(L^2_s \quad h^2\right)}{2h} = \sqrt{T_H^2 + T_z^2} \tag{19}$$

Maximum Tension (T$_{max}$)

$$T_{max} = T_H \times wh \tag{20}$$

Combing equations(18), (19)and (20) gives

$$L = h\sqrt{2\left(\frac{T_{max}}{wh}\right) - 1} \tag{21}$$

Hence, the minimum length required for mooring is

$$L_{min} = h\sqrt{2\left(\frac{T_{max}}{wh}\right) - 1} \tag{22}$$

whereT$_{max}$ ≤ T$_{br}$, andT$_{br}$is the breaking strength / tension in mooring line.Considering the horizontal distance x between anchor point A and the point where the lines touches the vessel. From figure 2 the following equation can be deduced to obtain the distance between anchor A and B.

$$X = L - L_s + x \tag{23}$$

$$X \ = \ L - h \ \sqrt{\left(1 + \frac{2a}{h}\right)} + a \cosh^{-1}\left(1 - \frac{h}{a}\right) \qquad (24)$$

$$X \ = \ L - h \ \sqrt{\left(\frac{1 - 2T_H}{wh}\right)} + \frac{T_H}{w} \cosh^{-1}\left(1 - \frac{wh}{T_H}\right) \qquad (25)$$

$$X \ = \ Cosh^{-1}\left(1 + \frac{h}{a}\right) \qquad (26)$$
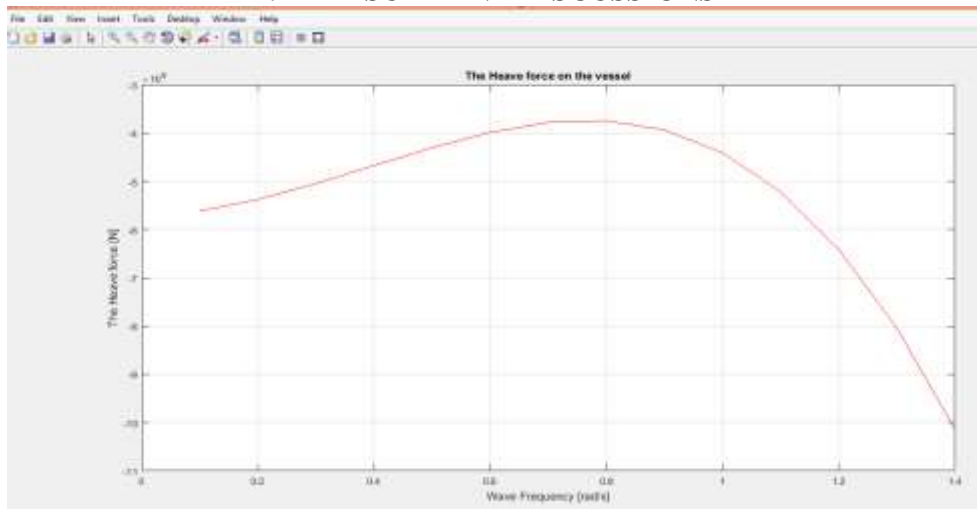
III.   RESULT AND DISCUSSIONS
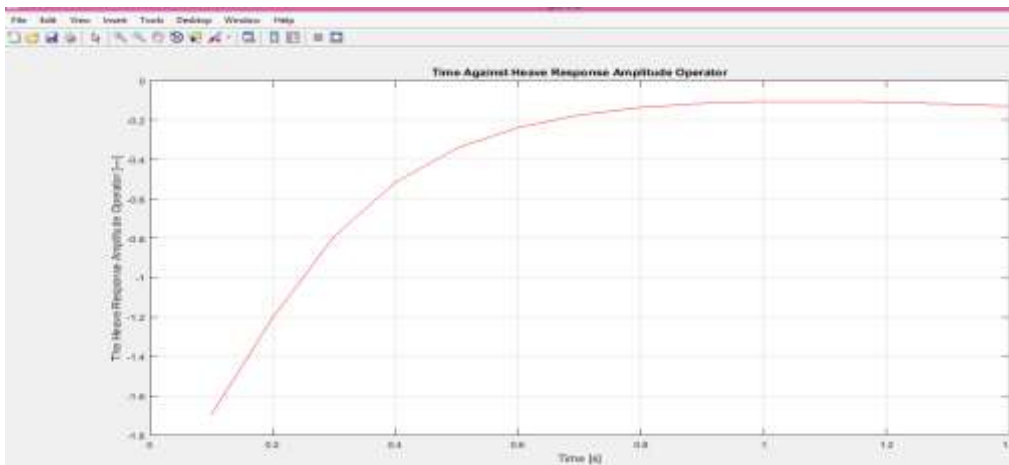

Figure 3: Wave Frequencies against Vessel Heave Force

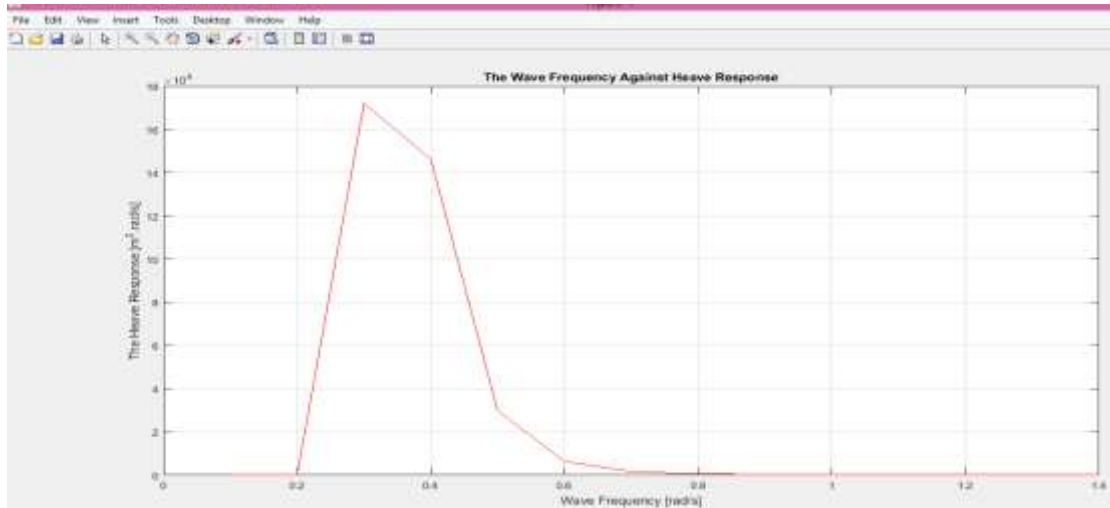**Figure 4: Wave Frequencies against Heave Response Amplitude Operator**

Figure 5: Wave Frequencies against Vessel Heave Responses
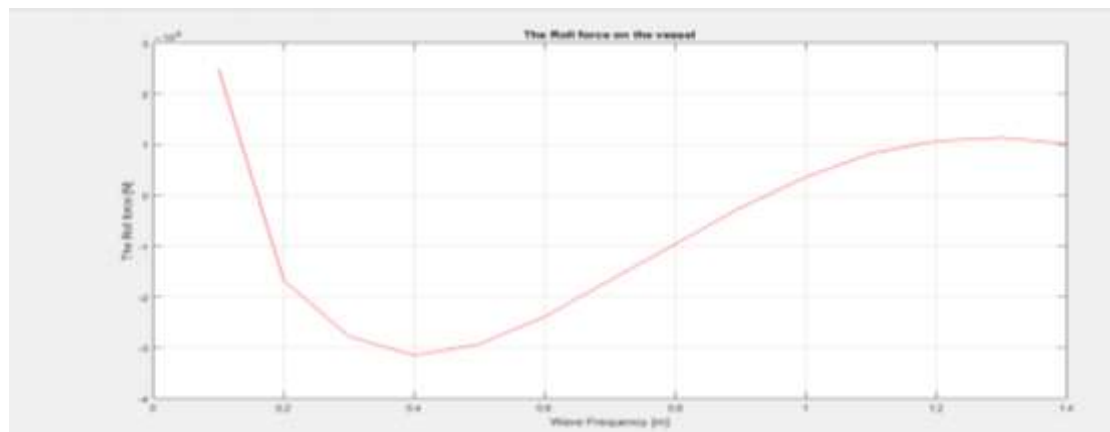
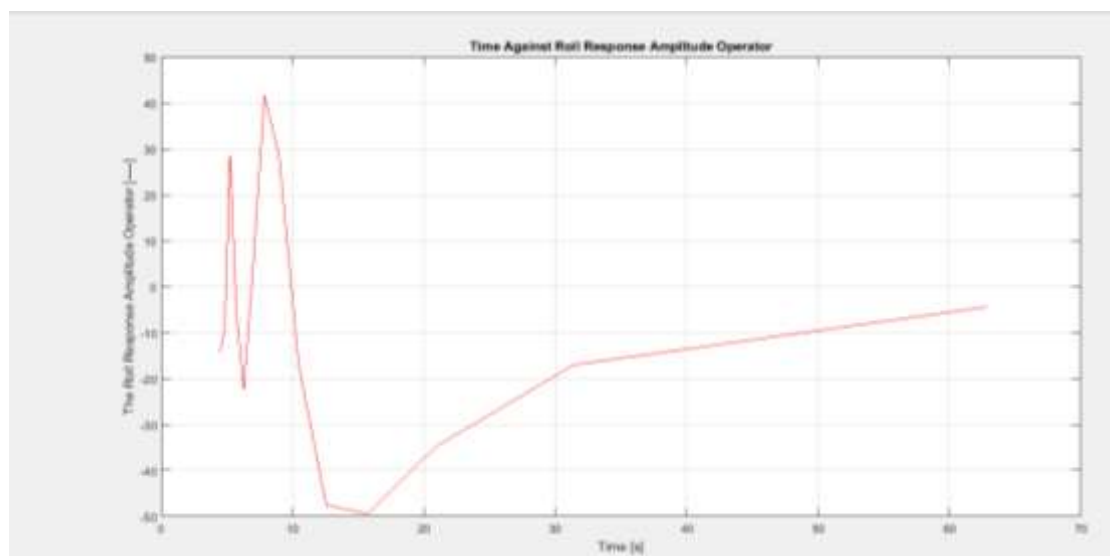**Figure 6: Wave Frequencies against Vessel Roll Force**

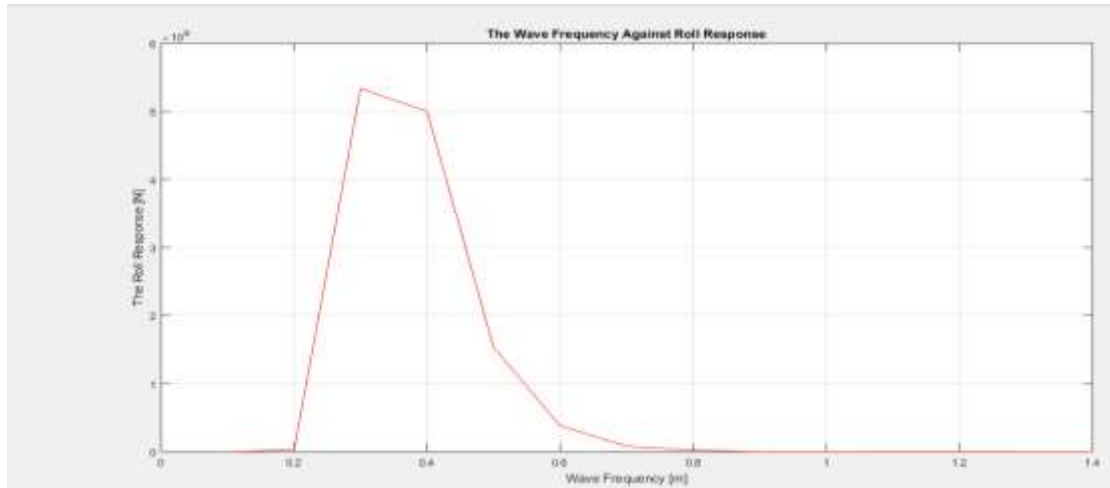**Figure 7: Roll Response Amplitude Operator against Time**

Figure 8: Wave Frequencies against Vessel Roll Responses
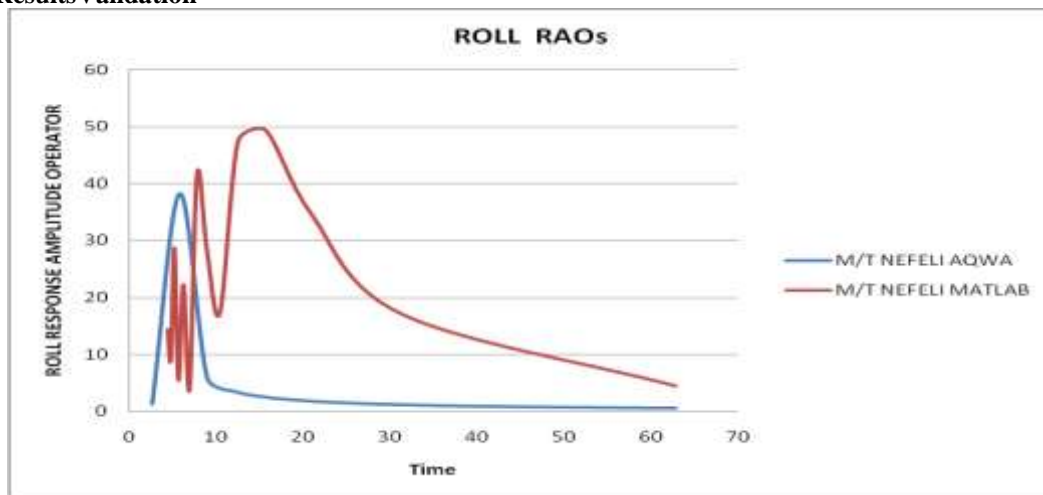
RAO ResultsValidation

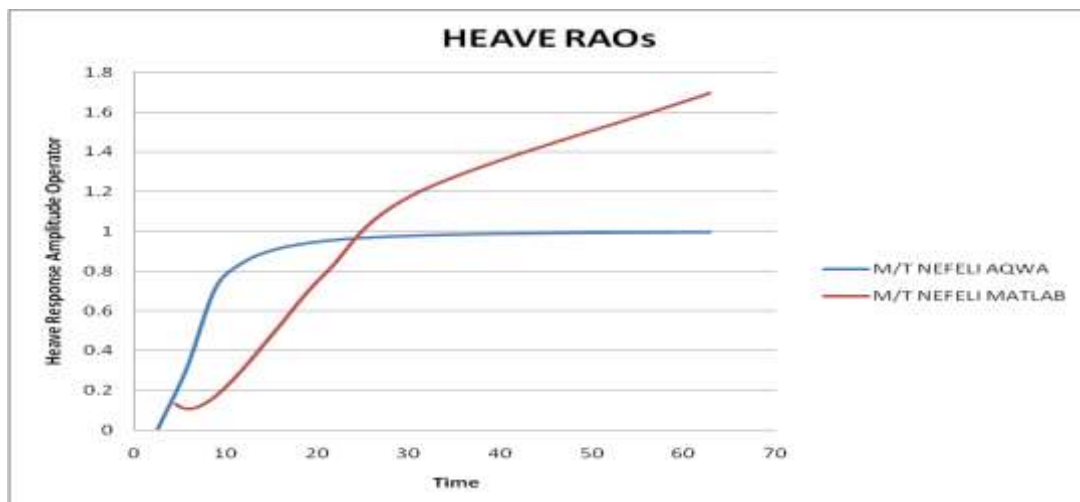**Figure 9: Roll Response Amplitude Operator Results Validation**

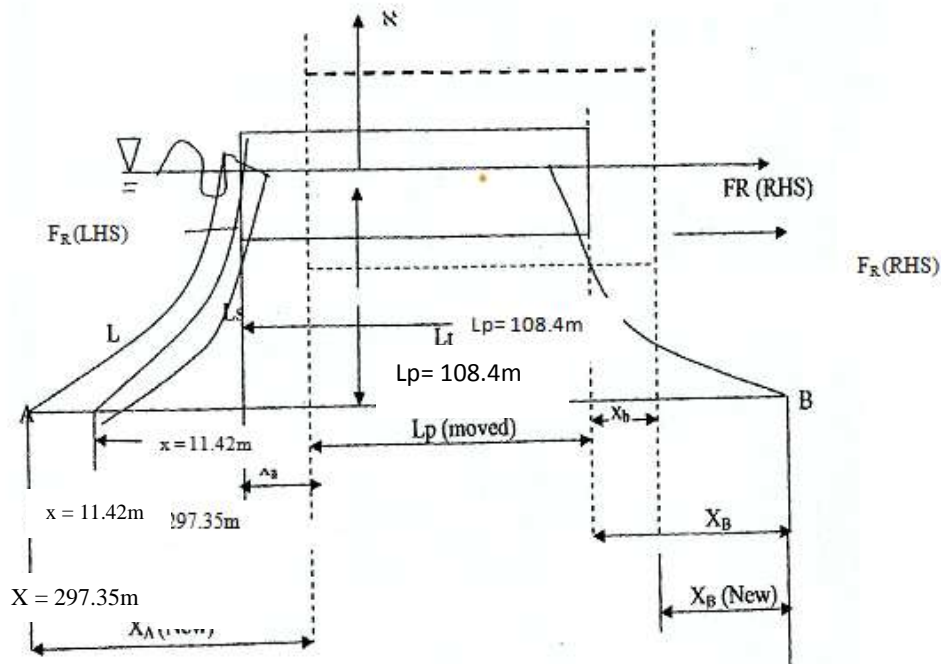**Figure 10: Heave Response Amplitude Operator Results Validation**

Figure 11: Environmental force on the platform to move anchor A

From the geometry of the above figure, X_a increases in XA as a result of environmental forces at the right-hand side, while X_B decreases in $X_B$due to the motion of the vessel in response to right hand side (RHS) environmental force to pull the anchor A. The force experienced on the vessel to pull anchor A is a right-hand side pulling force. Hence, the motion of the vessel stretches the tonedown point until the length of the Anchor line is fully extended to Anchor A. As the touch down length equals to the total length of the anchor line the vessel is equally displaced forward by an incremental amount X_a which is approximately equivalent to a reduction Xa towards anchor B. This implies that, $X_a = X_B$, and $L^s = L$

IV. DISCUSION

Figure 3 presents the plot of the heave force on the vessel against the wave frequency. The result shows that the heave force impact on the vessel increases gradually from zero beyond wave frequency of 0.45rad/s, the heave force drops swiftly to a local minimum of -2.7×10^{12}N at 1.0rad/s. The vessel at this point is visibly plunged into the sea and the magnitude of heave force is strongest. For frequencies higher than 1.0rad/s, the heave force grows steeply to 1.5×10^{12}N at 1.4rad/s. However, the heave impact is zero at frequencies 0.1, 0.55 and 13.5rad/s respectively.

Figure 4 shows the heave response amplitude operator plotted against wave frequency. The heave response amplitude operator determines the way the vessel will respond to the heave force as the wave frequency increases. The heave response amplitude operator is minimum at 0.1rad/s wave frequency. This is so because a still water vessel that suddenly experience load is bound to move rapidly in response to the sudden load impact. The heave response amplitude operator is maximum at 0.8rad/s and it continues to be at that maximum stage as the wave frequency increases from 1.0rad/s to 1.4rad/s.

Figure 5 displays the plot of vessel heave response against wave frequency. This defines the way the vessel reacts to the wave impact on the vessel. The vessel slightly responds in a way that is similar to the wave profile even though the vessel heave response is largely determined by heave response amplitude operator. As the wave frequency increases from 0.1rad/s to 0.2rad/s, the heave response remain at nearly zero. Just after 0.2rad/s, the vessel experiences a rapid heave response until it gets to maximum at 0.3rad/s. Then there is a rapid decrease of the heave response from maximum to zero as the wave frequency increases from0.3rad/s to 0.5rad/s. This is followed by a near zero heave response as the wave frequency increases from 0.5rad/sto 1.4rad/s.

Figure 6 presents the plot of the roll force on the vessel against the wave frequency, the results way similar to the wave profile. The roll force move from 2.5×10^9N to -1.5×10^9N as the wave current increases gradually from 0.1rad/s to 0.2rad/s, before the roll attain it maximum value of $-3.2 \times 10^9 N$ as the wave frequency move from 0.2rad/s to 0.4rad/s. Then the roll force begin to decline in negative direction as the wave

frequency increases from 0.4rad/s to 0.9rad/s,then the roll force attain an increase in the positive position as the wave frequency increases from 0.9rad/s to 1.4rad/s.

Figure 7 presents the plot of the roll response amplitude operator against wave frequency. The result determines the way the vessel respond to the roll force as the wave frequency increases to its positive maximum at 0.1rad/s. This is so because a still water vessel that suddenly experienced load, is bound to move rapidly to the sudden load impact. The roll response amplitude operator is maximum at 0.1rad/s with 1.4 value and it is maximum again at 0.4rad/s with about -27 value and this is the where the wave frequency has the maximum roll force. It is also observed that the roll response amplitude operator follows the pattern of the wave profile.

Figure 8 shows the vessel roll response against wave frequency. This defines the way the vessel reacts to the wave impacted on it. From thegraph, it shows that the vessel slightly respond in a way that is similar to that of the wave profile, even though the vessel roll response is largely determined by roll response amplitude operator.As the wave frequency increases from 0.1rad/s to 0.2rad/s, the roll response remain at nearly zero until just after 0.2rad/s when the vessel experience a rapid roll response until it get to maximum at 0.3rad/s. Then there is rapid decrease of the roll response from maximum to zero as the wave frequency increases gradually from 0.3rad/s to 0.8rad/s. This is then followed by a zero roll response as the wave frequency increases from 0.8rad/s to 1.4rad/s.

Figure 9 is the Roll Response Amplitude Operator result validation with the red plot showing the line of the Matlab results, while the blue line shown the AnsysAqwa result. When comparing both results (even though both result follow same part), it can be observed that the Matlab result is maximum at about $50\ ^m/_m$ while that of the Ansys Aqwa software is maximum at $40\ ^m/_m$. Also, the curve of the AnsysAqwa is linear enough while that of Matlab does not. This is due to the fact that while the Matlab was based on strip theory the AnsysAqwa was based on panel theory, and for the fact that the AnsysAqwa software make use of the overall length, beam and depth instead of the half breadth as used by the Matlab Source code.

V.   CONCLUSIONS

The results indicate that the heave force increases with varying wave frequency.The heave amplitude operator and the heave responses of the tanker decrease downwards with rising wave frequency.The maximum heave response occurs at region of maximum spectral density at same wave frequency. This is so because the spectral density carries the energy that is deposited on the tanker vessel and the vessel responses diminishes as wave frequency increases.Similarly, the surge force of the tanker vessel increases as wave frequency rises.The surge response amplitude operator follows in similar pattern. However, the surge response of the vessel follows a pattern similar to the wave spectral density as `shown with the graphs.The maximum surge responses $17 \times 10^5\ m^2 rad/_s$ occurs

at wave frequency of $0.5\ to\ 0.6\ ^{rad}/_s$ .Therefore, it can be concluded, that the results and validations that the source codes produced, if slightly improved upon and can be used for practical purpose.

REFERENCES
[1].   Huang, S. and Vassalos, D. (1993). A numerical method for predicting snap loading of marine cables, Appl. Ocean Res. 15,235-242.
[2].   Cozijn, J.L. and Bunnik, T.H.J.(2004). Coupled mooring analysis for a deep water calm buoy, Proceedings 23rd Int. Conf. Ocean Offshore Arctic Eng. OMAE 2004, Vancouver, Canada.
[3].   Hall M., Buckham, B. and Crawford, C., (2013). Evaluating the Importance of Mooring Line Model Fidelity in Floating Offshore Wind Turbine Simulations, Wind Energy.
[4].   Zhu K. Q., Zhu H. Y., Zhang Y. Z., Gao J., and Miao G. P., (2008). A Multi-Body Space-Coupled Motion Simulation for a Deep-Sea Tethered Remotely Operated Vehicle.
[5].   Zhu, K.Q., Zheng, D.C., Cai, Y., Yu, C.L., Wang, R., Liu, Y.L. & Zhang F., (2009). Nonlinear Hydrodynamic Response of Marine Cable-Body System under Random Dynamic Excitations, J. Hydrodyn. Ser. B 21(6), 851-855.
[6].   Lu W., Ge F., Wang L., Wu X., Hong Y., (2011). On the slack phenomena and snap force in tethers of submerged floating tunnels under wave conditions, Mar. Struct. 24(4), 258-376.
[7].   Han J. S., Son, Y. J., Choi, H. S., Rho J. B., (2011). The Transient Behavior of Mooring Systems in Line-Broken Condition, Proceedings 21st Int. Offshore and Polar Eng. Conf. ISOPE 2011, Maui, Hawaii.

[8].   Masciola M., Robertson A., Jonkman J., Coulling A. and Goupee A., 2013, Assessment of the Importance of Mooring Dynamics on the Global Response of the Deep C wind Floating Semisubmersible Offshore Wind Turbine, Proceedings 23rd Int. Offshore and Polar Eng. Conf., ISOPE 2013, Anchorage, Alaska, USA.

[9].   Minranj, C, A. (1982). Sea worthness: The forgotten Factor

[10].   Salseven, T. & Tucks, K.D. (2011). Ship motions and sea loads. 78, 250–287.

[11].   Lewis, F. (1968). The hydrodynamic coefficients for swaying, heaving and rolling cylinders in a free surface. International shipbuilding progress, vol.15, pp. 251-276.

[12].   Vugts, J. (1968). The hydrodynamic coefficient for swaying, heaving and rolling cylinders in a free surface. International shipbuilding progress, vol.15, pp. 251-276.

[13].   Bishop, R., Price, W. & Temarel, P. (1980). Hydrodynamic coefficients of some swaying and rolling cylinders of arbitrary shape. International shipbuilding progress, vol.27, pp. 54-65.

[14].   Ikeda, Y. (2004). Prediction methods of roll damping of ships and their application to determine optimum stabilization devices. Journals of Marine Technology, vol.41, no.2, pp. 89-93.

[15].   Muik, M.T.U. & Falzarano, J. (1994). Complex six degree of freedom nonlinear ship rolling motion. Journal of Offshore Mechanics and Arctic Engineering, vol.116, pp. 191-201.

[16].   Versteeg, H. & Malalasekera, M. (2007). An introduction to computational fluid dynamics using the finite volume method. 2nd editions, Prentice Hall.

[17].   Yeung, R., Liao, S.W. & Roddier, D. (1998). Hydrodynamic coefficients of rolling rectangular cylinders. International journal of Offshore and Polar Engineering, vol.8, no.4, pp. 241-250.

[18].   Yeung, R., & Ananthakrishnan, P. (1992). Oscillation of a floating body in a viscous fluid. Journal of Engineering Mathematic, vol.26, pp. 211-230.

[19].   Yeung, R., & Vajdhyanathan, M. (1994). Highly separated flows near a free surface.

[20].   Korpus, R. & Falzarano, J. (1997). Prediction of viscous ship roll damping by unsteady navier-stokes techniques. Journal of Offshore Mechanics and Arctic Engineering, vol.119, pp. 108-133.

[21].   Sarkar, T. & Vassalos, D. (2000). A RANS based technique for simulation of the flow near a rolling cylinder at the free surface. Journal of Marine Science and Technology, vol.5,pp. 66-77.

[22].   Kinnas, S., YU, Y.H. & Vinayan, V. (2006). Prediction of flows around FPSO hull sections in roll using an unsteady Navier-Stokes solvers. The international offshore society of offshore and polar Engineers conference, pp. 384-393.

[23].   Chen, H. & Liu, T. (2002). Time-domin simulation of large amplitude ship roll motions by Chimera RANS method. International Journal of Offshore and Polar Engineering, vol.12, no.3, pp. 206-212.

[24].   Wilson, R., Carrica, P. & Stern, F. (2006). Unsteady RANS method for ship motions with application to roll for a surface combatant. Journal of computers and fluids, vol.35, pp. 501-524.

[25].   Kim, K.H. (2003). Simulations of surface ship dynamics using unsteady RANS codes.

[26].   Lin, R.Q. & Kuang, W. (2008). Modeling nonlinear roll damping with a self consistent strongly nonlinear ship motion model. Journal of Marine Science and Technology, vol.13, pp. 127-137.

[27].   Querard, A. Yermarel, P.T. & Turnock, S. (2009). The hydrodynamics of ship like sections in heave, sway, and roll motions predicted using an unsteady Reynolds averaged navier-stokes method. Journal of Engineering for the Maritime Environment,

[28].   Bangun, E., Wang, C. & Utsunomiya, T. (2010). Hydrodynamic forces on a rolling barge with bilge keels. Applied ocean research, vol.32, no.2, pp. 219-232.

[29].   Ibrahim, R. & Grace, I. (2009). Modelling of ship roll dynamics and its coupling with heave and pitch. Vol.2010, no.1, pp. 1-32.